
SOFTENING, DAMAGE AND HIGHER-ORDER CONTINUA

René de Borst

Delft University of Technology, Faculty of Civil Engineering /

Eindhoven University of Technology, Faculty of Mechanical Engineering

Abstract

Simple, fracture-energy based and higher-order continuum concepts for simulating damage in quasi-brittle materials like concrete are introduced in a rather elementary fashion. A damage mechanics format is utilised for the elaboration, but this is not essential.

1 Problem statement

A basic problem when incorporating damage evolution, or more general, strain softening type constitutive relations, in standard continuum models is the inherent mesh dependence that is introduced by it. The conventional approach as well as novel features of recently proposed, enhanced continuum models are best demonstrated by the example of a simple bar loaded in uniaxial tension of Figure 1. Let the bar be divided into m elements. Prior to reaching the tensile strength f_t a linear relation is assumed between the normal stress σ and the normal strain ε :

$$\sigma = E\varepsilon, \tag{1}$$

with E Young's modulus. After reaching the peak strength a descending

slope is defined in this diagram through an affine transformation from the measured load-displacement curve. The result is given in Figure 2, where κ_u marks the point where the load-carrying capacity is totally exhausted. In the post-peak regime the constitutive model can thus be written as:

$$\sigma = f_t + h(\varepsilon - \kappa_0) . \quad (2)$$

In case of degrading materials $h < 0$ and h may be termed a softening modulus. For linear softening we have

$$h = - \frac{f_t}{\kappa_u - \kappa_0} . \quad (3)$$

Now suppose that one element has a tensile strength that is marginally below that of the other $m - 1$ elements. Upon reaching the tensile strength of this element failure will occur. In the other, neighbouring elements the tensile strength is not exceeded and they will unload elastically. Beyond the peak strength the average strain in the bar is then given by:

$$\bar{\varepsilon} = \frac{\sigma}{E} + \frac{E - h}{Eh} \frac{\sigma - f_t}{m} . \quad (4)$$

Substitution of expression (3) for the softening modulus h and introduction of n as the ratio between the strain κ_u at which the residual load-carrying capacity is exhausted and the threshold damage level κ_0 , $n = \kappa_u / \kappa_0$ and $h = -E/(n - 1)$, so that,

$$\bar{\varepsilon} = \frac{\sigma}{E} + \frac{n(f_t - \sigma)}{mE} . \quad (5)$$

The slope in the post-peak regime is then given by:

$$\frac{\dot{\bar{\varepsilon}}}{\dot{\sigma}} = \frac{1}{E} - \frac{n}{mE} . \quad (6)$$

The result is plotted in Figure 3 for different discretisations of the bar. We observe that there is a tremendous scatter in the results depending on the number of elements that is used. For $m = 1$ the input stress-strain diagram of Figure 2 is reproduced, but for $m = n$ the stress drops vertically after exceeding the tensile strength. For $m > n$ the average strain actually decreases after reaching the peak stress. This so-called snap-back behaviour implies that under quasi-static loadings not only the load, but also the displacement of the right end of the bar decreases. Experiments can no longer be kept stable under displacement control. Owing to the fact that

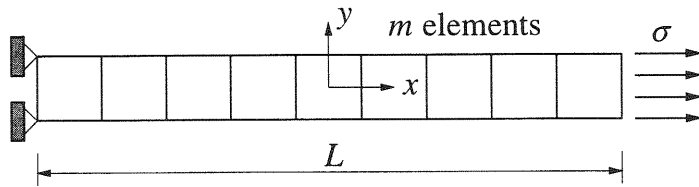


Fig. 1. Strain-softening bar subject to uniaxial loading.

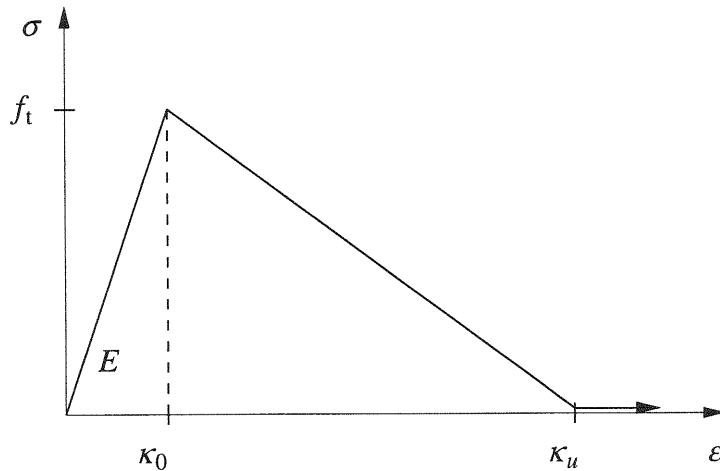


Fig. 2. Elastic-linear damaging material behaviour.

the localisation zone cannot absorb the elastic energy released in the unloading remaining parts of the bar, the observed failure of the specimen is of a highly explosive character.

The fact that a structure displays snap-back behaviour can be physical. However, the observation that eqs. (5) and (6) predict that for an infinite number of elements ($m \rightarrow \infty$) the post-peak curve doubles back on the original loading curve is suspect, since this implies that failure occurs without energy dissipation. From a physical point of view this is unacceptable and we must therefore either rephrase our constitutive model in terms of force-displacement relations, which implies the use of special interface elements (Schellekens 1992), or to enrich the continuum description by adding higher-order terms which can accommodate narrow zones of highly localised deformation quite similar to descriptions for boundary layers in fluids.

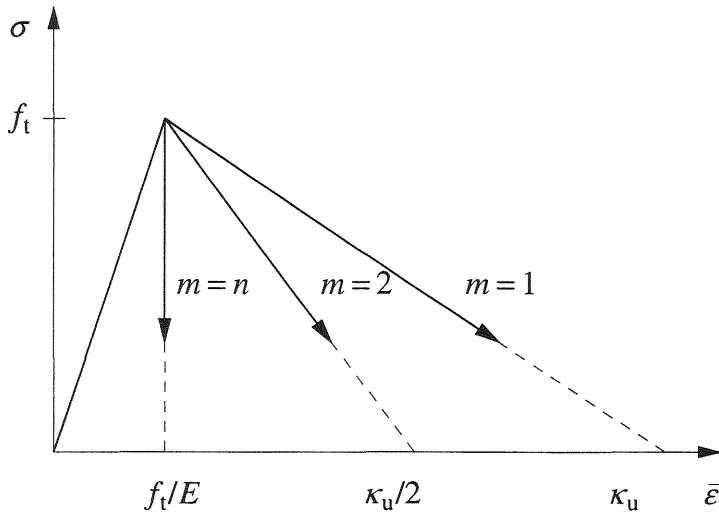


Fig. 3. Response of imperfect bar in terms of a stress-average strain curve.

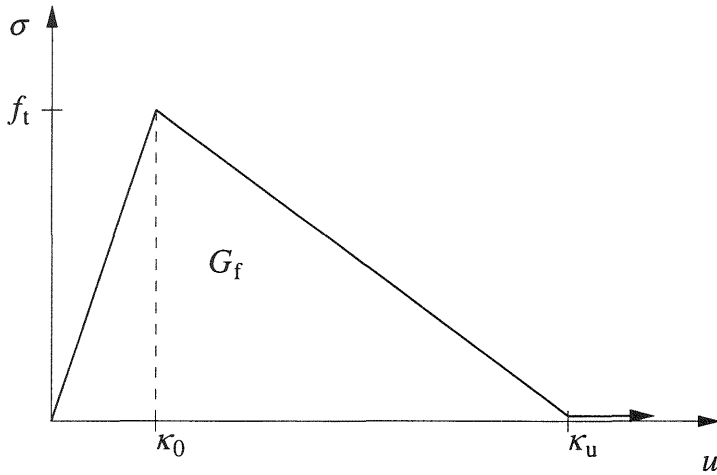


Fig. 4. Stress-displacement diagram for a bar.

2 Fracture energy based approaches

In an attempt to remedy a few of the most unpleasant features of the use of strain-softening models in a conventional continuum a number of authors (Pietruszczak and Mróz 1981, Bazant and Oh 1983, Willam 1984) have proposed to regard the area under the stress-displacement diagram of Figure 4 as a material parameter. This area represents the energy that is needed to create a unit area of a fully developed crack. It is commonly called the fracture energy and has the dimension of $[J/m^2]$ (equivalently, N/m). It

is noted that some authors only consider the part to the right of the damage threshold κ_0 as a material parameter in order to avoid a dependency on the value of the elastic properties (i.c. Young's modulus). Formally the definition of the fracture energy reads:

$$G_f = \int \sigma du = \int \sigma \varepsilon(s) ds . \quad (7)$$

with σ and u the stress and displacement over the cracked area. Assuming that localisation always occurs in one element - which, for lower-order elements, is confirmed by numerical experimentation - this idea has the consequence that the softening modulus h becomes a function of the element size. When the numerical calculation shows that the assumption of localisation in one element holds true, this approach indeed gives mesh insensitive results with regard to the value of the limit load and the shape of the load-displacement curve.

Carrying out the integration of eq. (7) for the linear softening diagram of Figure 4, and assuming that the strains are constant over the band width w (an assumption commonly made in numerical analyses), we arrive at the following relation between the strain κ_u at which the residual strength is exhausted, and G_f :

$$\kappa_u = \frac{2G_f}{f_t w} . \quad (8)$$

The softening modulus h is thus given by:

$$h = - \frac{w f_t^2}{2G_f - f_t^2 w / E} . \quad (9)$$

Making use of the observation that $w = L / m$, with L the length of the bar (Figure 1), the expression for the softening modulus becomes:

$$h = - \frac{L f_t^2}{2m G_f - L f_t^2 / E} . \quad (10)$$

We observe that this pseudo-softening modulus is proportional to the structural size and inversely proportional to the number of elements.

We shall now carry out an analysis for the tension bar of Figure 1 and give one element a tensile strength marginally below the other elements. As with the stress-based fracture model of the previous section the average strain in the post-peak regime is given by eq. (4). However, substitution of the fracture-energy based expression (10) for the pseudo-softening modulus h now results in:

$$\bar{\epsilon} = \frac{\sigma}{E} + \frac{2G_f(f_t - \sigma)}{Lf_t^2} \quad (11)$$

so that beyond the peak stress the tangential relation between the stress rate $\dot{\sigma}$ and the average strain rate $\dot{\bar{\epsilon}}$ reads:

$$\frac{\dot{\bar{\epsilon}}}{\dot{\sigma}} = \frac{1}{E} - \frac{2G_f}{Lf_t^2}. \quad (12)$$

We observe that, in contrast to the pure stress-based fracture model, the number of elements has disappeared from the expressions for the ultimate average strain and the slope of the stress-average strain curve. Therefore, the results in terms of stress-average strain curves, or alternatively, of load-displacement curves, are insensitive with regard to mesh refinement. Eqs. (11) and (12) show that the inclusion of the fracture energy G_f as a material parameter eliminates the spurious mesh dependence, since the number of elements m has disappeared from the expressions for $\bar{\epsilon}$ and the slope of the descending branch $\dot{\bar{\epsilon}}/\dot{\sigma}$. But also the specimen length L enters the expression for $\bar{\epsilon}$. In other words, the brittleness of the structure now depends upon the value of L , so that, effectively, a size effect is introduced. Indeed, for large values of L the second term of eq. (11), which is always non-negative, approaches zero. $\bar{\epsilon}$ becomes smaller and smaller and in the limiting case that $L \rightarrow \infty$, $\bar{\epsilon} \rightarrow \sigma/E$, which means that the stress-average strain curve doubles back on its original loading branch.

3 Non-local continuum models

Although good results can be obtained with fracture-energy based approaches, in the sense that mesh-insensitive results can be obtained with regard to the limit load, the method remains something of a ‘trick’. This becomes apparent when considering that this approach leaves the width of the localisation zone unspecified or when studying a localisation zone that propagates through the mesh in a zig-zag manner. Indeed, energy-based fracture models are just a first step to model failure phenomena within the framework of a smeared concept that goes beyond the classical idea of a ‘simple material’. A more elegant and mathematically sounder approach is to introduce additional terms in the continuum description which reflect the changes in the micro-structure that occur during failure processes. The result is that the boundary value problem remains well-posed also during fracture and that a proper description is achieved of the localisation process accompanying failure. For instance, the width of the fracture process zone is contained in the mathematical description and is no longer one ele-

ment wide as in numerical simulations of fracture in a conventional continuum. When the elements are taken smaller than the width of the fracture process zone, localisation occurs in more than one element.

A simple way to depart from the concept of a ‘simple solid’ is to modify eq. (2) which states that the residual stress beyond peak load is exclusively a function of the strain in the material point itself. Instead, one could write:

$$\sigma = f_t + h (\tilde{\varepsilon} - \kappa_0) , \quad (13)$$

where $\tilde{\varepsilon}$ is defined by the integral expression

$$\tilde{\varepsilon} = \int_{-L/2}^{L/2} g(s)\varepsilon(x+s)ds , \quad (14)$$

with L the length of the bar (Figure 1) and $g(s)$ a weighting function. While this expression can be generalised to three dimensions (Pijaudier-Cabot and Bazant 1987, Mühlhaus and Aifantis 1991) this will not be done here to preserve transparency of the treatment. The error function is a possible choice for $g(s)$ that meets the intuitive notion that the non-local character of a constitutive law as eq. (14) should fade away rapidly for larger distances. Then eq. (14) changes into

$$\tilde{\varepsilon} = \int_{-L/2}^{L/2} \frac{1}{2l\sqrt{\pi}} \exp(-s^2/4l^2)\varepsilon(x+s)ds , \quad (15)$$

where l is a characteristic material parameter with the dimension of length that can be related to the size of the softening zone.

Several alternative formulations have been considered in the literature, which have essentially the same effect as eqs (14) and (15). For instance, one could rephrase eq. (2) by introducing a ‘plastic’ strain

$$\varepsilon^p = \varepsilon - \sigma/E \quad (16)$$

to arrive at a nonlocal plasticity model. Setting $h' = Eh/(E - h)$, the result is given by

$$\sigma = f_t + h' \tilde{\varepsilon}^p \quad (17)$$

where the plastic strain is averaged over the domain:

$$\tilde{\varepsilon}^p = \int_{-L/2}^{L/2} \frac{1}{2l\sqrt{\pi}} \exp(-s^2/4l^2) \varepsilon^p(x+s) ds . \quad (18)$$

4 Gradient continuum models

When $\varepsilon(x+s)$ is developed in a Taylor series around $s=0$, we obtain instead of eq. (15):

$$\begin{aligned} \tilde{\varepsilon} = & \int_{-L/2}^{L/2} \frac{1}{2l\sqrt{\pi}} \exp(-s^2/4l^2) \varepsilon(x) ds + \int_{-L/2}^{L/2} \frac{s}{2l\sqrt{\pi}} \exp(-s^2/4l^2) \frac{d\varepsilon(x)}{dx} ds \\ & + \int_{-L/2}^{L/2} \frac{s^2}{4l\sqrt{\pi}} \exp(-s^2/4l^2) \frac{d^2\varepsilon(x)}{dx^2} ds + \dots \end{aligned} \quad (19)$$

If it is assumed that $L \gg l$ (which implies that the structural size is several orders of magnitude larger than the size of the localisation zone) and if higher-order terms are neglected the integrals of eq. (19) can be evaluated analytically. The result is

$$\tilde{\varepsilon} = \varepsilon + l^2 \frac{d^2\varepsilon}{dx^2} . \quad (20)$$

With expression (20), eq. (13) can be replaced by:

$$\sigma = f_t + h(\varepsilon - \kappa_0) + hl^2 \frac{d^2\varepsilon}{dx^2} . \quad (21)$$

It is noted that the second term on the right-hand of eq. (19) cancels in the integration process. More generally all odd derivatives of ε with respect to x cancel upon integration over the entire bar. Extension of eq. (2) to include just the first gradient of the strain (Schreyer and Chen 1986) therefore seems less natural. In sum, gradient models as defined in eq. (21) can be derived from non-local models by expanding the kernel of the integral employed in the averaging procedure for the strains. It is remarked that the gradient term can act as a stabiliser if and only if $h < 0$. This implies that the gradient term as introduced in eq. (21) would indeed be stabilising in the softening regime, but would be destabilising in case of hardening, which would be neither physically meaningful, nor computationally desirable. Therefore the more general expression

$$\sigma = f_t + h(\varepsilon - \kappa_0) - c \frac{d^2 \varepsilon}{dx^2} \quad (22)$$

is used instead of eq. (21), with $c > 0$ a material constant. Similarly, a formulation like

$$\sigma = f_t + h' \varepsilon^p - c \frac{d^2 \varepsilon^p}{dx^2} \quad (23)$$

can be conceived for gradient-dependent plasticity (cf. eq. (17)).

When compared to the original non-local formulation as expressed through eqs. (13) and (14) the gradient model (22) has two important advantages:

- It is computationally much more efficient, as for the gradient models an efficient algorithm can be developed that satisfies the evolution equation for the inelastic strains in a distributed sense.
- The additional boundary conditions on the inelastic strains which have to be enforced in non-local and gradient continuum models can be formulated uniquely and elegantly for gradient models. Indeed, for gradient plasticity models the non-standard boundary conditions can be derived from a variational principle.

The properties of non-local and gradient continuum models can most lucidly be brought out by constructing analytical solutions. For the bar of Figure 1 and considering the 2nd grade material as defined by eq. (23) a closed-form solution exists which shows that, when a steady-state solution has developed, the width of the fracture process zone is given by (de Borst and Mühlhaus 1992):

$$w = 2\pi l, \quad (24)$$

while the slope in the diagram in which the stress σ versus the average strain $\bar{\varepsilon}$ is given, reads:

$$\frac{\dot{\bar{\varepsilon}}}{\dot{\sigma}} = \frac{1}{E} + \frac{2\pi l}{Lh'}. \quad (25)$$

Comparing expression (25), which results from a one-dimensional gradient model, and eq. (12) shows that the fracture-energy based model can give the same result as the gradient model, in the sense that the same slope in the stress-displacement diagram is computed, when

$$G_f = - \frac{\pi l f_t^2}{h'} . \quad (26)$$

It is emphasised that in eq. (26) h' is the softening modulus in the gradient model and not the size-dependent softening modulus in the fracture energy model. When we substitute the tensile strength f_t and the softening modulus h' used in the numerical analyses and take $l = 10$ mm we obtain $G_f = 0.0628$ N/mm, which, for a linear softening diagram, is a commonly accepted value for normal-weight concrete. Also the width $w = 62.8$ mm which follows from eq. (24) reasonably agrees with data reported in the literature which suggest that $w \approx 3d_a$ (Bazant and Pijaudier-Cabot 1989). Of course, many crude assumptions have been made in deriving this correspondence, e.g., the adopted linear shape of the softening curve and, in the G_f -model, the homogeneous distribution of the strains over the localisation zone. The above coarse analysis nevertheless gives an indication on the range of values for the length parameter l in the gradient model.

5 References

- Bazant, Z.P. and Oh, B. (1983) Crack band theory for fracture of concrete. **RILEM Mater. Struct.**, 16, 155-177.
- Bazant, Z.P. and Pijaudier-Cabot, G. (1989) Measurement of characteristic length of nonlocal continuum. **ASCE J. Eng. Mech.**, 115, 755-767.
- de Borst, R. and Mühlhaus, H.-B. (1992) Gradient-dependent plasticity: formulation and algorithmic aspects. **Int. J. Num. Meth. Eng.**, 35, 521-539.
- Mühlhaus, H.-B. and Aifantis, E.C. (1991) A variational principle for gradient plasticity. **Int. J. Solids Structures**, 28, 845-858.
- Pietruszczak, S. and Mróz, Z. (1981) Finite element analysis of deformation of strain softening materials. **Int. J. Num. Meth. Eng.**, 17, 327-334.
- Pijaudier-Cabot, G. and Bazant, Z.P. (1987) Nonlocal damage theory. **ASCE J. Eng. Mech.**, 113, 1512-1533.
- Schellekens, J.C.J. (1992) **Computational Strategies for Composite Structures**. Dissertation, Delft University of Technology, Delft.
- Schreyer, H.L. and Chen, Z. (1986) One-dimensional softening with localization. **J. Appl. Mech.**, 53, 791-979.
- Willam, K.J. (1984) Experimental and computational aspects of concrete fracture, in **Proc. Int. Conf. Computer Aided Analysis and Design of Concrete Structures** (eds F. Damjanić et al.), Pineridge Press, Swansea, Part 1, 33-70.